EurJIC
European Journal of Inorganic Chemistry

Research Article
doi.org/10.1002/ejic.202300286

Chemistry Europe
European Chemical Societies Publishing

www.eurjic.org

Special Collection

Bis(chlorido)tin(IV)*meso*-substituted Porphyrins-Characterization and Solubility

Doris M. Grössl,[a] Anna-Viktoria Hafner,[a] Roland C. Fischer,[a] Robert Saf,[b] Ana Torvisco,*[a] and Frank Uhlig[a]

Dedicated to Professor Rainer Streubel in celebration of his scientific contributions

Investigation of the solubility behavior of *para*-substituted (H, Me, *t*-Bu, *n*-Bu) *meso*-tetraarylporphyrins as well as *meso*-tetraalkylporphyrins (Me, *n*-Pr, *n*-Bu) were performed. An increase of solubility in chloroform and benzene is detected according to the higher functionality in *para* position of the phenyl ring for *meso*-tetraarylporphyrins or in *meso* position on *meso*-tetraalkylporphyrins. Furthermore, the series of bis(chlorido)tin(IV) *meso*-tetraarylporphyrin and bis(chlorido)tin(IV) *meso*-tetraalkylporphyrin was investigated via UV/Vis spectroscopy, ^{119}Sn-NMR and single crystal X-ray diffraction.

Introduction

Porphyrins play an important role in many biological functions[1,2] and their optical functionality, design flexibility and structural properties make them important materials for industrial and medical applications.[3] Further enhancing these optical properties is the introduction of highly charged group 14 metal centers into the porphyrin ring which do not disturb the planarity of the ring.[2,4–6] Specifically, tin(IV) porphyrins with trans-diaxial ligands can be manipulated to achieve a large variety of these complexes[6] which have applications ranging from catalysts,[7] photodynamic therapy for cancer treatments,[8] to antimicrobial textiles.[9] Useful starting materials for functionalization of the trans-diaxial ligands in tin porphyrin systems are the bis(chlorido)tin(IV) *meso*-tetrasubstituted porphyrin derivatives.

While the synthesis of bis(chlorido)tin(IV) *meso*-tetraarylporphyrin compounds has been extensively studied and well described in literature,[10] their solid state characterization has been more intriguing. Aside from bis(chlorido)tin(IV) *meso*-tetraphenylporphyrin, only few structurally characterized *meso* aryl-substituted species are reported in literature and either contain electron withdrawing or donating groups (Figure 1). However, it should also be noted that several bis(chlorido)tin(IV) *meso*-tetra(*para*-substituted-aryl)substituted porphyrins (*p*-tolyl, *p*-ethyl-C_6H_4, *p*-*t*-butyl-C_6H_4)[11–15] have been prepared, but are not completely structurally characterized by single crystal X-ray diffraction. In the case of *meso*-tetraalkyl substituted tin(IV) porphyrins, only the bis(chlorido)(*meso*-tetraheptylporphyrinato)tin(IV) has been previously published by Martelli et al.[16] The compound was also not structurally characterized by single crystal X-ray diffraction.

For all literature known free base *meso*-tetrasubstituted porphyrins and bis(chlorido)tin(IV) *meso*-tetrasubstituted porphyrin complexes, limited solubility in common organic solvents occurs, and therefore hindering their application. The solubility of the free base porphyrins has been shown to depend on *meso*- vs *ß*-substituent position, number and nature of the substituent (alkyl, aryl).[17] Thus far, solubility studies for metal containing porphyrin complexes have been limited. A

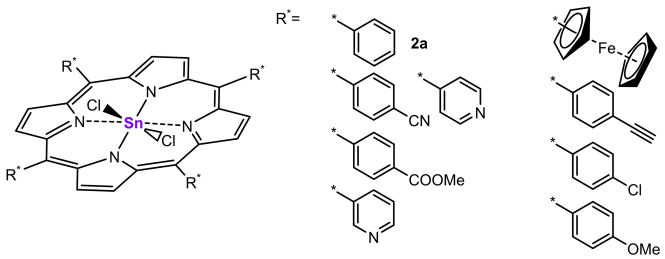

Figure 1. Literature known structurally characterized by single crystal XRD bis(chlorido)(*meso*-tetraR*porphyrinato) tin(IV) compounds[20,21–24]

[a] D. M. Grössl, A.-V. Hafner, Prof. R. C. Fischer, Dr. A. Torvisco, Prof. F. Uhlig
Graz University of Technology
Institute of Inorganic Chemistry
Stremayrgasse 9/IV
8010 Graz (Austria)
E-mail: ana.torviscogomez@tugraz.at

[b] Prof. R. Saf
Graz University of Technology
Institute for Chemistry and
Technology of Materials
Stremayrgasse 9/V
8010 Graz (Austria)

Supporting information for this article is available on the WWW under https://doi.org/10.1002/ejic.202300286

Special Collection Part of the celebratory collection for Rainer Streubel

Research Article
doi.org/10.1002/ejic.202300286

DFT investigation of the solubility of *meso*-substituted zinc porphyrins[18] was reported, as well as, a solubility study of ß-substituted nickel and vanadium porphyrin complexes.[19] However, to the best of our knowledge no conclusive studies on comparing the substituents effects of the free *meso*-tetrasubstituted porphyrins or bis(chlorido)tin(IV) *meso*-tetrasubstituted porphyrin derivatives have been reported thus far.

Therefore, the focus of this work is on the synthesis and characterization via UV/Vis, as well as, single crystal X-ray diffraction of *para*-substituted (H, Me, *t*-Bu, *n*-Bu) *meso*-tetraarylporphyrins in addition to the more neglected *meso*-tetraalkylporphyrins (Me, *n*-Pr, *n*-Bu). The goal of this work was the enhancement of the solubility for not only the free base porphyrins but especially the bis(chlorido)tin(IV) species by varying the nature (alkyl, aryl) of the substituents.

Results and Discussion

Synthesis of meso-tetraR*porphyrins (1 a–1 g)

The preparation of free base porphyrins has been discussed thoroughly in literature.[2] The aforementioned *meso*-tetraarylporphyrins **1 b**, **1 c** and **1 d** were prepared via the Adler method first published in 1964.[25] Equimolar amounts of pyrrole and the respective aldehyde were refluxed in propionic acid for 1 h. Following yields were achieved: 23 % for **1 b**, 21 % **for 1 c** and 18 % for **1 d**. The products were obtained as blueish purple powders with metallic hue (Scheme 1). **1 a** (97 %) was purchased by ABCR GmbH & Co KG.

The discussed *meso*-tetraalkylporphyrins **1 e, 1 f** and **1 g** were synthesized according to the Lindsey Method.[26] In this reaction, equimolar amounts of pyrrole and the respective aldehyde are brought to react in dry dichloromethane with BF_3*OEt_2 to obtain the porphyrinogen. After oxidation with *p*-chloranil, the synthesized *meso*-tetraalkylporphyrins were purified by column chromatography and received with yields of 7 % for **1 e**, 10 % for **1 f** and 12 % for **1 g**. **1 e**–**1 g** were obtained as reddish-purple powders.

Synthesis of bis(chlorido)(meso-tetraR*porphyrinato) tin(IV) (2 a–2 g)

The synthesis of **2 a**–**2 g** was performed as previously reported.[10,11,13,14] However, a different work up procedure was employed,[4] where the reaction mixture was centrifuged after cooling to RT at 2000 rpm for 30 minutes and the solution decanted. The remaining slurry was dissolved in chloroform and purified via filtration from excess $SnCl_2 \cdot 2H_2O$. While the synthesis of **2 a**–**2 c** is well described in literature,[10–14] the synthesis of **2 d**–**2 g** has not been mentioned so far to the best of our knowledge. **2 e** precipitated after addition of water as a dark purple powder, which could not be re-dissolved again in an abundance of common organic solvents. All novel compounds were characterized by ^{1}H-NMR, ^{119}Sn-NMR, UV/Vis as well as, MALDI-TOF-MS.

Attempts to enhance the solubility

An important aspect of employing these compounds in applications, such as bulk-heterojunction solar cells, is their solubility. Enhancing the solubility might prove beneficial towards higher thickness and more consistent morphology and distribution of the active layer in bulk-hetero junction solar cells as shown by preliminary results in previously reported work.[27] Therefore, it is worthwhile exploring the effect of the R* group.

The solubility studies of the aforementioned free base porphyrins (**1 a**–**1 f**) were performed in chloroform, benzene, DME and heptane (see Figure 2). All free base porphyrins showed an extreme low solubility in heptane of < 1 mmol L^{-1}. The solubility in DME was also significantly lower than in chloroform and benzene. Although **1 a** does not follow the trend, one can see that for **1 b** to **1 d** and **1 e** to **1 g** the solubility

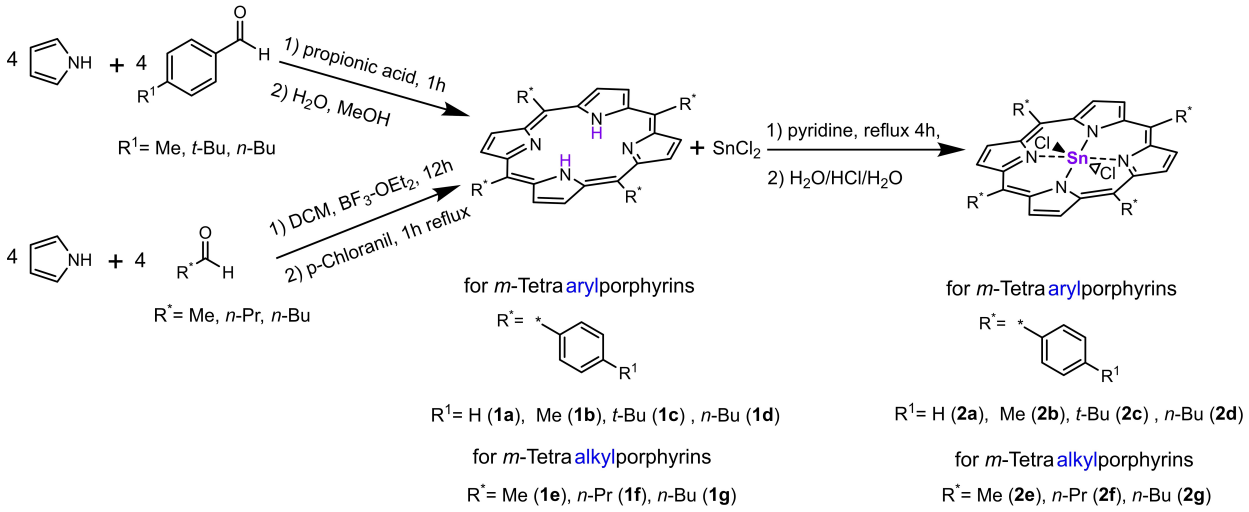

Scheme 1. Synthetic paths towards compounds **1 a**–**1 g** and **2 a**–**2 g**.

Research Article
doi.org/10.1002/ejic.202300286

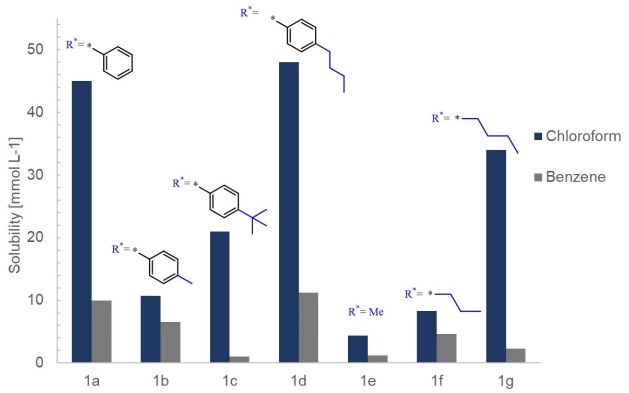

Figure 2. Solubility of **1a**–**1g** in chloroform and benzene in mmol L^{-1}.

in chloroform increases with an increase of the alkyl chain. Solubility of all free base porphyrins(**1a**–**1g**) showed higher solubility in chloroform on average compared to benzene, with the longest chain **1d** showing the highest solubility with 48 mmol L^{-1} in chloroform.

The solubility studies of **2a**–**2g** were performed in chloroform and benzene (Figure 3). Since the solubility in heptane and DME was overall extremely low, these solvents are not further discussed here. In general, we see that the free base porphyrins **1a**–**1g** have a higher solubility as compared to the bis(chloride)tin(IV) compounds, **2a**–**2g**.

In the case of bis(chlorido)tin(IV) *meso*-tetraalkylporphyrins (Me, *n*-Pr, *n*-Bu) (**2e**–**2g**), poor solubility was observed in benzene (< 1 mmol L^{-1}) with only a slight increase of solubility in chloroform. The highest solubility was observed for the *n*-butyl substituted **2g** with 7 mmol L^{-1} in chloroform.

Solubility is drastically increasing moving from the *meso*-tetraalkylpoprhyrins (**2e**–**2g**) to the *meso*-tetraarylporphyrins (**2a**–**2d**). Replacement of the alkyl groups by aryl moieties (**2a**–**2d**) in the *meso* position, resulted in an increase in solubility both benzene (4–13 mmol L^{-1}) and chloroform (15–34 mmol L^{-1}).This was also observed for the free base porphyrins.

In accordance with higher chain length on the *para* position of the phenyl group, the solubility increases from **2a** to **2d**. The exception is **2c** with a slightly higher solubility in benzene of 13 mmol L^{-1} as compared to **2d** with 11 mmol L^{-1}. The highest solubility could be achieved for **2d** with 34 mmol L^{-1} in chloroform. For the *meso*-tetraalkylporphyrins (**2e**–**2g**), a similar trend can be observed. As mentioned above, **2e** precipitated out of the reaction solution upon formation and could not be redissolved in quantitative amounts in an abundance of several common organic solvents. **2f** and **2g** were slightly more soluble with 2 mmol L^{-1} in chloroform for **2f** and 7 mmol L^{-1} in chloroform for **2g**. Due to the solubility increase (19 mmol L^{-1}) afforded by **2d**, exchanging the previously used **2a**[27] with **2d**, as the starting material for bulk-hetero junction solar cells, has the potential to improve their performance.

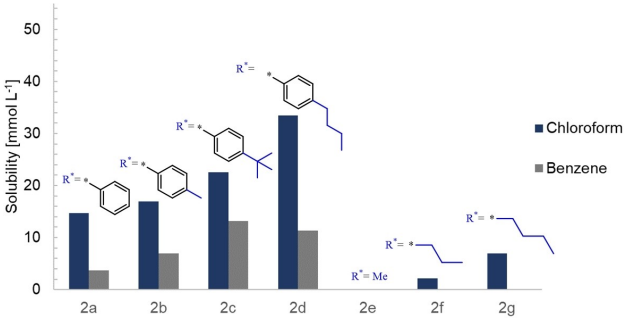

Figure 3. Solubility of **2a**–**2g** in chloroform and benzene in mmol L^{-1}.

Characterization via NMR

NMR measurements were performed either in $CDCl_3$ or C_6D_6 at room temperature. ^{1}H-NMR shifts fall within the expected ranges for these porphyrins and are as described in literature.[28,29,30] ^{119}Sn-NMR shifts for **2a**–**2g** are about −588 ± 1 ppm, which is typical for these compounds. For compounds **2f** and **2g**, the ^{119}Sn-NMR shift could not be obtained via direct measurement of solution ^{119}Sn-NMR due to low solubility. However, 2D-^{1}H-^{119}Sn HMBC-NMR succeeded to give the ^{119}Sn-NMR shifts of −587 ppm for both **2f** and **2g**.

Also, solution state ^{1}H-NMR of **2e** was not successful due to the extremely low solubility in common organic solvents. To confirm the synthesis of **2e**, ^{119}Sn-MAS-NMR was performed for **2e** and chemically similar **2f** and **2g**. This resulted in ^{119}Sn-MAS-NMR shifts of −588 ppm for **2e** and −591 ppm for both **2f** as well as **2g** (see Figure 4). Therefore, it can be concluded that the synthesis of **2e** was successful. A comparison of the solution ^{119}Sn-NMR of **2e** and **2f** to the ^{119}Sn-MAS-NMR show that these results are consistent as shown in Table 1. Although some of the described porphyrins are well known in literature, ^{13}C-NMR

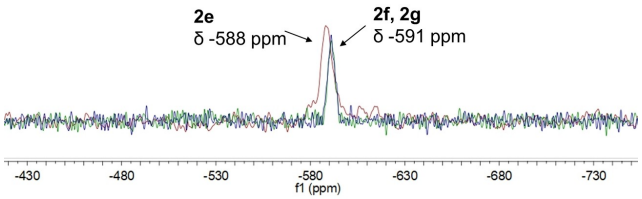

Figure 4. ^{119}Sn-MAS-NMR of Cl_2SnTMeP(**2e**) in comparison to Cl_2SnT*n*-BuP(**2f**) & Cl_2SnT*n*-PrP(**2g**).

Table 1. Solution and solid state ^{119}Sn-NMR shifts of **2a**–**2g**.

Nr.	Compound	^{119}Sn-NMR	^{119}Sn-MAS-NMR
2a	Cl_2SnTPP	−588	–
2b	Cl_2SnTTP	−588	–
2c	Cl_2SnT*t*-BuPP	−587	–
2d	Cl_2SnT*n*-BuPP	−588	–
2e	Cl_2SnTMeP	–	−588
2f	Cl_2SnT*n*-PrP	−587	−591
2g	Cl_2SnT*n*-BuP	−587	−591

Research Article
doi.org/10.1002/ejic.202300286

investigations have been sometimes lacking. The distinction between sp^2-hybridized carbon atoms (150–120 ppm) and *sp*-hybridized carbon atoms (50–10 ppm) can be easily made, an exact assignment of the shifts to the corresponding carbon atoms is however more difficult. ^{13}C-NMR of **2b**–**2d** and **2f**–**2g** showed a ^{119}Sn-^{13}C coupling of 30 Hz at the shift of 130 ppm.

UV/Vis Spectroscopy

Apart from ^{1}H-NMR und ^{119}Sn-NMR spectroscopy, the UV/Vis absorption behaviour is an excellent analytical tool for porphyrin chemistry. Figure 5 and Figure 6 show the UV/Vis absorption data for the selected compounds **1b**, **1d**, **1e** and **1g**. The spectra were recorded in benzene and the maxima are normalized to 1. The same trend can be observed for the same substance classes. Variation of the alkyl group in either the *para* position of the phenyl group for *meso*-tetraarylporphyrins. (**1a**–**1d, 2a**–**2d**) or in the *meso* position of the porphyrin ring for *meso*-tetraalkylporphyrins (**1e**–**1g, 2e**–**2g**) does not affect the absorption behaviour. Comparison of the absorption maxima shows a slight bathochromic shift of 1–4 nm for the *meso*-tetraarylporphyrins (**1a**–**1d**) with 421 nm as compared to the *meso*-tetraalkylporphyrins (**1e**–**1g**) with 417 nm. The bis(chlorido)tin(IV) species **2a**–**2g** are bathochromic shifted as compared to the free base porphyrins **1a**–**1g**. **2a**–**2d** have an absorption maximum of 430 nm, whereas **2e**–**2g** have an absorption maximum at 429 nm. Due to the poor solubility of **2e**, a saturated solution of **2e** was centrifuged and filtered prior to measurement.

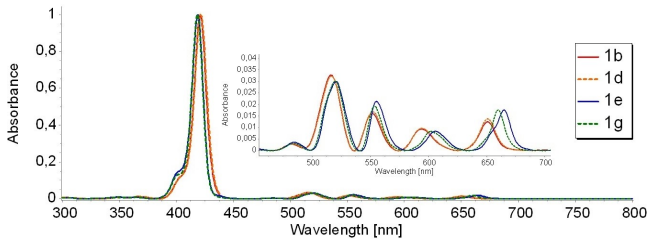

Figure 5. UV-Vis absorption spectra for **1b**, **1d**, **1e**, **1g** in benzene, [λ] wavelength (nm), [E] rel.Int.(1).

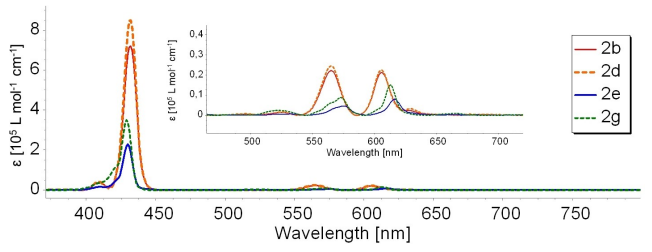

Figure 6. UV-Vis absorption spectra for **2b**, **2d**, **2e**, **2g** in benzene, [λ] wavelength (nm), ε [10^5 L mol^{-1} cm^{-1}].

Single crystal X-Ray Diffraction

Structurally characterized *meso*-tetraaryl and *meso*-tetraalkyl freebase porphyrins are well known in literature.[28,30,31] However, less structural information is available on the corresponding bis(chlorido)tin(IV) *meso*-tetra substituted porphyrin derivatives, due to difficulties in isolating pure products, and as discussed above, low solubility in common organic solvents. Only the bis(chlorido)tin(IV) *meso*-tetra substituted porphyrins containing either electron donating or withdrawing groups mentioned in Figure 1 were structurally characterized by single crystal X-ray Diffraction. While the synthesis of compounds **2a**–**2c** have been previously reported,[10–14] only bis(chlorido)tin(IV) *meso*-tetra*phenyl*porphyrin **2a** has been structurally characterized. Dissolving **2b**–**2d** in chloroform only lead to successful crystallization of the newly prepared **2d** as purple blocks (Figure 7). In contrast to **2d**, compounds **2b** and **2c** did not yield X-ray quality crystals even after various attempts and combinations of solvent systems. It was only possible to obtain solid state structures of compound **2b** and **2c** as co-crystals after crystallization in toluene by slow evaporation in the presence of naphthalene. **2b** was crystallized as red blocks, while **2c** was crystallized as purple blocks. Despite the addition of different alkyl chain lengths on the *para* position on the phenyl ring of the porphyrin, compounds **2a**–**2d** are structurally similar. Characteristic bond lengths and angles of all compounds structurally characterized via single crystal X-ray diffraction are listed in Table 2.

As mentioned above, in contrast to the bis(chlorido)tin(IV) *meso*-tetra*aryl*porphyrins no bis(chlorido)tin(IV) *meso*-tetra*alkyl*-porphyrins have been structurally characterized. Due to its low solubility (< 1 mmol L^{-1}) (Figure 3) and regardless of multiple attempts, good quality crystals of **2e** were not able to be obtained. However, X-ray quality crystals for the first structurally characterized bis(chlorido)tin(IV) *meso*-tetraalkylporphyrins (**2f** and **2g**) were achieved by slow evaporation in chloroform as green or purple blocks. As can be seen in Table 2, there is no substantial structural deviation to the core porphyrin ring by changing the group on the *meso* position. Correlating with the higher degree of rotation of the alkyl chains in the *meso* position in **2f** and **2g**, disorder is observed in the propyl and butyl chains around the terminal alkyl chains, respectively. In the bis(chlorido)tin(IV) *meso*-tetraarylporphyrins, disorder was only observed in **2c** around the *para t*-butyl group on the phenyl ring. In the extended solid state, compounds **2b**–**d**, **2f**–**g** display a series of both non-covalent electrostatic interactions in the form of C–H···π packing interactions through the central

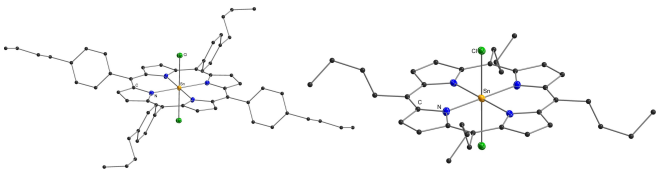

Figure 7. Crystal structure diagram for **2d** (left) and **2g** (right). All non-carbon atoms shown as 30% shaded ellipsoids. Hydrogen atoms omitted for clarity.

Research Article
doi.org/10.1002/ejic.202300286

Table 2. Selected bond lengths [Å] and angles [°] for **2a**–**2d** and **2f**–**2g**.

	2a[24]	**2b**	**2c**	**2d**	**2f**	**2g**
Sn–Cl	2.420(1)	2.444(2)	2.4007(13)	2.4250(11)	2.4631(4)	2.460(2)
Sn–N′	2.098(2)	2.099(6)	2.091(3)	2.090(3)	2.0915(12)	2.095(7)
Sn–N″	2.098	2.099(5)	2.091(3)	2.101(3)	2.0940(13)	2.100(7)
Cl–Sn–Cl	180.0	180.0	180.0	180.0	180.0	180.0
N′–Sn–Cl	90.0	89.93(19)	90.0	89.58(9)	90.75(4)	90.000(1)
N″–Sn–Cl	90.0	90.94(16)	90.0	89.64(9)	89.82(4)	88.8(2)

Table 3. Table of interactions (values in [Å]) in the extended solid state for presented bis(chlorido)tin(IV) *meso*-tetraarylporphyrins (**2a**–**2d**, **2f**–**2g**) and reported values for literature known bis(chlorido)tin(IV) *meso*-tetraarylporphyrins.

Substance	C–H···Cl	(methyl) C–H···pyrrole	(methyl) C–H···aryl	(aryl) C–H···pyrrole	(pyrrole) C–H···aryl
2a[24]	3.06	–	–	2.94	–
2b	2.82–3.11	–	3.28	2.97–3.12	2.74–2.83
2c	3.17–3.35	2.83–3.40	–	–	–
2d	2.76–3.18	–	2.91	2.78–3.01	2.14–3.41
2f	2.91–3.10	–	–	–	–
2g	2.82	2.98–3.13	–	–	–
***p*-COOMe**[23]	–	–	–	2.76–2.88	–
***p*-pyridine**[21]	2.71	–	–	–	–
***p*-OMe**[22]	2.78	–	–	–	–

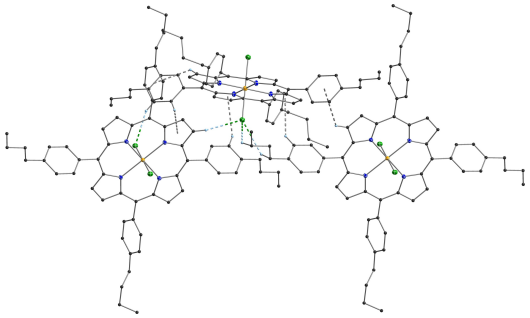

Figure 8. Crystal packing diagram for **2d** C–H···π interactions and C–H···Cl contacts highlighted by dashed bonds. All non-carbon atoms shown as 30% shaded ellipsoids. Hydrogen atoms not involved in intermolecular interactions omitted for clarity.

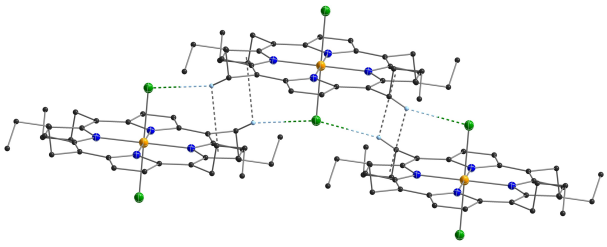

Figure 9. Crystal packing diagram for **2g**. C–H···π interactions and C–H···Cl contacts highlighted by dashed bonds. All non-carbon atoms shown as 30% shaded ellipsoids. Hydrogen atoms not involved in intermolecular interactions omitted for clarity.

porphyrin ring and aryl substituents between neighbouring molecules, as well as, C–H···Cl contacts (Table 3, Figure 8, Figure 9). The interactions observed for **2b**–**d**, **2f**–**g** are in range for reported to C–H···π[32,33,34] and C–H···Cl[35,36–38] values and compare nicely to values reported for literature known bis(chlorido)tin(IV) *meso*-tetraarylporphyrins[22–24,39] (Table 3). These also fall within range of C–H···π interaction (2.85–3.05 Å) and C–H···Cl interactions (2.64–3.35 Å) as reported for a series of structurally similar bis(chlorido)tin(IV) *meso*-triarylcorroles.[40]

Conclusions

Classically, bis(chlorido)tin(IV)porphyrins have shown low solubility hindering their application. In order to evaluate materials with increased solubility for example in bulk-heterojunction solar cell applications, a series of literature known and novel *meso*-tetraaryl- and *meso*-tetraalkyl- free base porphyrins and bis(chlorido)tin(IV) *meso*-tetraaryl- and *meso*-tetraalkylporphyrins with varying R* moieties at the *meso* position were prepared. For these studies, literature known bis(chlorido)tin(IV) *para*-substituted (H, Me, *t*-Bu) *meso*-tetraarylporphyrins (**2a**–**2c**), as well as, newly reported bis(chlorido)tin(IV) *para*-substituted *meso*-tetra(*n*-butylphenyl)porphyrin (**2d**) and bis(chlorido)tin(IV) *meso*-tetraalkylporphyrins (Me, *n*-Pr, *n*-Bu) (**2e**–**2g**) were prepared and characterized. The solubility of the free base

Research Article
doi.org/10.1002/ejic.202300286

porphyrins and the respective bis(chlorido)tin(IV) derivatives were evaluated relative to the nature and length of the R* moiety, as well as compared to the respective free base porphyrins. *Meso*-tetraalkylporphyrins are generally less soluble than *para*-substituted *meso*-tetraarylporphyrins. For both alkyl- and aryl-substituted porphyrins, overall solubility increases with the longer chain length on the *para* position with **2 d** as the most soluble. Therefore, this makes **2 d** the best candidate for future employment of tin(IV) porphyrins in applications such as in bulk-heterojunction solar cells, where enhancement of the solubility of the bis(chlorido)tin(IV) *meso*-tetrasubstitutedporphyrins could prove beneficial.

Experimental Section

General Procedures: All reactions were carried out under argon using common Schlenk techniques. Flasks were flame-dried before its use. Argon 5.0 was used as received. Organic solvents were dried via a solvent drying system from Innovative Technology Inc. DCM was purchased from VWR Int. dried with P_4O_{10}, distilled and stored in Schlenk flasks. Deuterated solvents were (C_6D_6, $CDCl_3$) were purchased from Deutero GmbH and dried with standard procedures. H_2TPP(**1 a**) 97% was purchased from ABCR GmbH & Co KG and used as received. *n*-BuLi (1.6 M in hexane) and $BF_3 \cdot OEt_2$ (48%) were purchased from Acros organics. $SnCl_2 \cdot 2H_2O$ was purchased from Riedel de Haën. Pyridine and propionic acid were purchased from Merck Millipore KGaA. Pyrrol, *p*-Chloranil and all used aldehydes were purchased from Sigma Aldrich and used as received.

Elemental Analysis was performed on a VARIO micro cube (Heraeus Elementar) for CHN.

NMR Measurements were acquired either on a RS^{2}D 300 MHz spectrometer (^{1}H: 300 MHz, ^{119}Sn: 111.8 MHz, ^{13}C:75.5 MHz) or on a RS^{2}D 400 MHz spectrometer (^{1}H:400 MHz, ^{119}Sn:149 MHz, ^{13}C:100.6 MHz). As reference TMS ($\delta = 0$ ppm) was used for ^{1}H-NMR and ^{13}C-NMR, Me_4Sn ($\delta = 0$ ppm) for ^{119}Sn-NMR. ^{119}Sn-MAS-NMR spectra under magic angle spinning (MAS) conditions were recorded on a 500 MHz Avance spectrometer (Bruker) with a nominal magnetic field of 11.7 T.

UV/Vis Measurements were performed at a "Cary 60 UV-VIS" from "Agilent Technologies". F. Menges "Spectragryph - optical spectroscopy software", Version 1.2.16, 2022, http://www.effemm2.de/spectragryph/ was used for illustration. Due to the poor solubility of **2 e**, a saturated solution of **2 e** in benzene was centrifuged for 1 h at 2000 rpm and filtered through a 0.20 μm CHROMAFIL® Xtra PTFE-20/25 filter prior to measurement.

Electron ionization (EI+, 70 eV, source at 250 °C) mass spectra were acquired on a JMS–T2000GC (AccuTOFTM GC-Alpha) from JEOL Ltd. (Tokyo, Japan) equipped with a direct insertion probe (DIP). 0.5 μL of a solution of the sample (c = 0.05 mg/mL in $CHCl_3$) were placed in the glass cup used for DIP, dried under ambient conditions, and transferred into the vacuum. Mass spectra were continuously acquired (mass range: 50–750 Da; 2.5 spectra/s; resolution: appr. 30000 FWHM) while the sample was heated from room temperature to 450 °C. Data were processed using msAxel (version 4.0).

MALDI-TOF mass spectrometry was performed on a Waters micro MX time-of-flight mass spectrometer. Ions were generated by irradiation just above the threshold laser power (laser: wavelength 337 nm, operated at a frequency of 5 Hz). Positive ion spectra were recorded in reflectron mode and externally calibrated with a suitable mixture of poly(ethyleneglycol)s (PEG). The spectra of appr. 100–150 shots were averaged. Samples were prepared by mixing a solution of DCTB (c = 10 mg/mL in $CHCl_3$) and a solution of the sample (c = 0.05 mg/mL in $CHCl_3$) in the cap of a microtube in a ratio of 10:1 (v/v). 0.5 μL of the resulting mixture were deposited on the sample plate (stainless steel) and allowed to dry under ambient conditions. Analysis of data was done with MassLynx 4.1.

Single crystal X-ray Crystallography

Deposition Number(s) 2262999 (**1 d**), 2263000 (**2 b**), 2263001 (**2 c**), 2263002 (**2 d**), 2263003 (**2 f**), 2263004 (**2 g**) contain(s) the supplementary crystallographic data for this paper. These data are provided free of charge by the joint Cambridge Crystallographic Data Centre and Fachinformationszentrum Karlsruhe Access Structures service.

Further information on single crystal X-ray crystallography can be found in the supporting information.

Synthesis of 1 b–1 d: 190 ml of propionic acid was transferred into a three neck round bottom flask and heated to reflux, then simultaneously, 5 ml of pyrrole (0.072 mol, 1 eq.) and 0.074 mol (1.03 eq.) of the respective aldehyde were added dropwise. A color change from yellow to dark red/purple was observed. The reaction was kept under reflux for 1 h. After cooling to RT, the product precipitated and was filtered off. Residual side products were removed by washing with 200 ml hot deionized water and 300 ml methanol.

Synthesis of 1 e–1 g: 10.5 ml pyrrole (1 eq., 0.15 mol) and 0.15 mol of the respective aldehyde were added to 1 L of dry DCM and purged with argon for 30 min. Then, 3.5 ml of boron trifluoride etherate (28 mmol) was added dropwise and stirred overnight. After adding 27.7 g *p*-Chloranil (0.11 mol), the mixture was refluxed for 1 h. After cooling to RT, the mixture was run through an alumina column and further purified via column chromatography on alumina using dichloromethane/cyclohexane.

Synthesis of 2 a-2 g: 1.70 mmol of the corresponding free base porphyrin and 5.1 mmol $SnCl_2 \cdot 2H_2O$ were added into a round bottom flask and dissolved in 100 ml of pyridine. Afterwards, the reaction mixture was refluxed for 4 h. A color change from purple to greenish/blue was observed. After cooling to RT, 100 ml of deionized H_2O was added to the crude product and stirred for 15 minutes. The precipitate is then separated by centrifugation at 2000 rpm for 20 minutes. Afterwards the precipitate was washed with 100 ml deion. H_2O, 100 ml 6 M HCl and 100 ml deion. H_2O. The precipitate was dissolved in $CHCl_3$, filtered and the solvent removed via rotary evaporation. This resulted in an amorphous purple powder.

All synthesized compounds were decomposed after 300 °C (mp (Decomposition): > 300 °C).

Solubility Measurements: Solubility measurements were performed by preparing a highly saturated solution of the porphyrins in chloroform, benzene, DME and heptane. Then 5–20 ml of solution were filtered through a 0.20 μm CHROMAFIL® Xtra PTFE-20/25 filter and pumped to complete dryness and weighed via a Kern ALS200-4 scale. Standard deviation was less than 5% for all compounds.

Experimental data for **1 a**–**1 g** and **2 a**–**2 c** are according to literature.[2,10–14]

Dichloro[5,10,15,20-tetra(4-butylphenyl)porphyrinato]tinIV (Cl_2SnT*n*-BuPP, 2 d): Isolated yield: 65% (1.11 mmol) purple powder recrystallized from chloroform to give purple blocks for single crystal XRD

^{1}H-NMR (300 MHz, C_6D_6): δ 9.21 (s, $^{4}J_{SnH}$ 14.88 Hz, 8H; β-pyrrolic-H); 8.21 (d, $^{3}J_{HH}$ 7.5 Hz, 8H; Ar-*o*-H); 7.61 (d, $^{3}J_{HH}$ 8.3 Hz, 8H; Ar-*m*-H); 2.99 (t, 8H; C**H**$_2$CH$_2$CH$_2$CH$_3$); 1.95 (tt, 8H; CH$_2$C**H**$_2$CH$_2$CH$_3$); 1.62 (qt, 8H; CH$_2$CH$_2$C**H**$_2$CH$_3$); 1.12 ppm (t, 12H; CH$_2$CH$_2$CH$_2$C**H**$_3$);

^{119}Sn-NMR (111.8 MHz, C_6D_6): δ −588 ppm (s); ^{13}C-NMR (100.6 MHz, $CDCl_3$): 146.5 (s), 143.3 (s), 138.0 (s), 135.0 (s), 132.7 (s, $^{3}J_{SnC}$ 15.4 Hz), 127.1 (s), 121.3 (s), 35.8 (s), 33.8 (s), 22.7 (s), 14.2 ppm (s); UV/Vis (C_6H_6, λ(nm)/ε [10^5 L mol^{-1} cm^{-1}]): 410/0.39, 430/8.50, 565/0.24, 605/0.22; elemental analysis calcd (%) for $C_{60}H_{60}Cl_2N_4Sn$: C 70.19, H 5.89, N 5.46; found: C 70.22, H 5.88, N 5.35; MALDI-TOF-MS(DCTB) m/z (%): 1026.34 [M$^+$ req 1026.32], 991.35 (100) [(M–Cl)$^+$ req 991.35];

Dichloro[5,10,15,20-tetra(methyl)porphyrinato]tinIV (Cl_2SnTMeP, 2e): Isolated yield: 60% (1.02 mmol) blueish grey powder

^{119}Sn (MAS-NMR, referenced to SnO_2 at −604 ppm): δ −588 ppm (s) UV/Vis (C_6H_6, λ(nm)/ε [10^5 L mol^{-1} cm^{-1}]): 408/0.14, 429/2.50, 575/0.05, 616/0.08; elemental analysis calcd (%) for $C_{24}H_{20}Cl_2N_4Sn$: C 52.03, H 3.64, N 10.11; found: C 50.11, H 3.40, N 7.32; MALDI-TOF-MS(DCTB) m/z (%): 554.01 [M$^+$ req 554.01], 519.04 [(M–Cl)$^+$ req 519.04];

Dichloro[5,10,15,20-tetra(*n*–propyl)porphyrinato]tinIV (Cl_2SnT*n*-PrP, 2f): Isolated yield: 60% (1.02 mmol) purple powder recrystallized from chloroform to give green blocks for single crystal XRD

^{1}H-NMR (400 MHz, $CDCl_3$): δ 9.84 (s, $^{4}J_{SnH}$ 15.86 Hz, 8H; β-pyrrolic-H), 5.12 (t, 8H, C**H**$_2$CH$_2$CH$_3$), 2.73 (q, 8H; CH$_2$C**H**$_2$CH$_3$), 1.40 ppm (t, J_{CH} 106 Hz, 12H; CH$_2$CH$_2$C**H**$_3$); ^{13}C-NMR (100.6 MHz, $CDCl_3$): 146.2(s), 130.5 (s, $^{3}J_{SnC}$ 34.13 Hz), 120.6 (s), 38.7 (s), 38.6 (s), 15.8 ppm (s); 2D-^{1}H-^{119}Sn-HMBC-NMR (149 MHz, C_6D_6): δ −587 ppm (s) ^{119}Sn (MAS-NMR, referenced to SnO_2 at −604 ppm): δ −591 ppm (s) UV/Vis (C_6H_6, λ(nm)/ε [10^5 L mol^{-1} cm^{-1}]): 408/0.24, 429/3.98, 572/0.09, 612/0.15; elemental analysis calcd (%) $C_{32}H_{36}Cl_2N_4Sn$: C 57.69, H 5.45, N 8.41; found: C 56.63, H 5.49, N 7.71; MALDI-TOF-MS(DCTB) m/z (%): 666.13 [M$^+$ req 666.13], 631.16 (100) [(M–Cl)$^+$ req 631.17]; DIP-MS (EI+, 70 eV, source at 250 °C) m/z: 666.1326 [M$^+$ req 666.1327], 631.1641 [(M–Cl)$^+$ req 631.1644], 596.1968 [(M-2Cl)$^+$ req 596.1963];

Dichloro[5,10,15,20-tetra(*n*-butyl)porphyrinato]tinIV (Cl_2SnT*n*-BuP, 2g): Isolated yield: 65% (1.11 mmol) purple powder recrystallized from chloroform to give purple blocks for single crystal XRD

^{1}H-NMR (400 MHz, $CDCl_3$): δ 9.85 (s, $^{4}J_{SnH}$ 14.33 Hz, 8H; β-pyrrolic-H), 5.14 (t, 8H, C**H**$_2$CH$_2$CH$_2$CH$_3$), 1.91 (tt, 8H; CH$_2$C**H**$_2$CH$_2$CH$_3$), 1.21 (qt, 8H; CH$_2$CH$_2$C**H**$_2$CH$_3$), 1.19 ppm (t, 12H; CH$_2$CH$_2$CH$_2$C**H**$_3$);^{13}C-NMR (100.6 MHz, $CDCl_3$): δ 145.6 (s), 129.9 (s, $^{3}J_{SnC}$ 28.7 Hz), 120.3 (s), 41.3 (s), 36.1 (s), 24.0 (s), 14.4 ppm (s); 2D-^{1}H-^{119}Sn-HMBC (149 MHz, C_6D_6): δ −587 ppm (s) ^{119}Sn (MAS-NMR, referenced to SnO_2 at −604 ppm): δ −591 ppm (s) UV/Vis (C_6H_6/ε [10^5 L mol^{-1} cm^{-1}]): 422/0.34, 429/3.50, 523/0.25, 573/0.09, 613/0.15; elemental analysis calcd (%) $C_{36}H_{44}Cl_2N_4Sn$: C 59.86, H 6.14, N 7.79; found: C 57.74, H 6.07, N 7.20 M; MALDI-TOF-MS(DCTB) m/z (%): 722.20 [M$^+$ req 722.20], 687.23 (100) [(M–Cl)$^+$ req 687.23]; DIP-MS (EI+, 70 eV, source at 250 °C) m/z: 722.1930 [M$^+$ req 722.1954], 687.2244 [(M–Cl)$^+$ req 687.2271], 652.2575 [(M-2Cl)$^+$ req 652.2590];

Supporting Information

Additional references cited within the Supporting Information.[41–56]

Acknowledgements

The authors gratefully acknowledge the ^{119}Sn-MAS-NMR measurements performed by Katharina Hogrefe (AG Wilkening). The support by the "Jeol Application Lab" at Graz University of Technology is gratefully acknowledged. The authors are grateful to the Graz University of Technology and the NAWI Graz project for financial support.

Conflict of Interests

The authors declare no conflict of interest.

Data Availability Statement

The data that support the findings of this study are available in the supplementary material of this article.

Keywords: NMR spectroscopy · porphyrinato tin(IV) · solubility · tin · UV/Vis absorption · X-ray diffractionv

[1] a) F. Bryden, R. W. Boyle, *Insights from Imaging in Bioinorganic Chemistry*, Academic Press, Cambridge, **2016**; b) M. Momenteau, C. A. Reed, *Chem. Rev.* **1994**, *94*, 659.
[2] K. M. Kadish *Handbook of porphyrin science. With applications to chemistry, physics, materials science, engineering, biology and medicine*, World Scientific, Singapore, **2010**.
[3] Y. Shi, F. Zhang, R. J. Linhardt, *Dyes Pigm.* **2021**, *188*, 109136.
[4] S. Stadlbauer, R. Fischer, M. Flock, P. W. Zach, S. M. Borisov, A. Torvisco, F. Uhlig, *Z. Naturforsch. B* **2017**, *72*, 801.
[5] S. Stadlbauer, D. Grössl, R. Fischer, N. Demitri, F. Uhlig, *J. Organomet. Chem.* **2020**, *925*, 121470.
[6] D. P. Arnold, J. Blok, *Coord. Chem. Rev.* **2004**, *248*, 299.
[7] a) C. J. Medforth, Z. Wang, K. E. Martin, Y. Song, J. L. Jacobsen, J. A. Shelnutt, *Chem. Commun.* **2009**, *47*, 7261; b) Y. Yang, Q. Wang, Z. Su, J. Li, N. Wang, *Eur. J. Inorg. Chem.* **2023**, *26*.
[8] B. W. Pogue, B. Ortel, N. Chen, R. W. Redmond, T. Hasan, *Cancer res.* **2001**, *61*(2), 717.
[9] G. Sun, (Ed.) *Antimicrobial textiles*, Woodhead Publishing, **2016**.
[10] M. J. Crossley, P. Thordarson, R. A.-S. Wu, *J. Chem. Soc. Perkin Trans. 1* **2001**, *18*, 2294.
[11] E. R. Baral, D. Kim, S. Lee, M. H. Park, J. G. Kim, *Catal.* **2019**, *9*, 311.
[12] S. Wang, C. Forsyth, S. J. Langford, *CrystEngComm* **2015**, *17*, 3060.
[13] J. Chen, L. K. Woo, *Inorg. Chem.* **1998**, *37*, 3269.
[14] M. M. Rahman, K. Hassan, K. Hirabayashi, S. Sato, T. Shimizu, K.-i. Sugiura, *Polyhedron* **2019**, *171*, 128.
[15] F. Espitia-Almeida, C. Díaz-Uribe, W. Vallejo, D. Gómez-Camargo, A. R. Romero Bohórquez, *Molecules* **2020**, *25*, 1887.
[16] C. Martelli, J. Canning, J. R. Reimers, M. Sintic, D. Stocks, T. Khoury, M. J. Crossley, *J. Am. Chem. Soc.* **2009**, *131*, 2925.
[17] G. Mamardashvili, N. Mamardashvili, B. Berezin, *Molecules* **2000**, *5*, 762.
[18] K. Sanusi, O. C. Atewolara-Odule, N. O. Sanyaolu, A. A. Ibikunle, P. B. Khoza, N. O. Fatomi, S. A. Fasanya, H. E. Abuka, E. O. Jesugbile, Y. Yilmaz, *Struct. Chem.* **2023**, *34*, 891.
[19] D. H. Freeman, I. D. Swahn, P. Hambright, *Energy Fuels* **1990**, *4*, 699.
[20] a) T. Lang, E. Graf, N. Kyritsakas, M. W. Hosseini, *Dalton Trans.* **2011**, *40*, 3517; b) P. V. Solntsev, B. D. Neisen, J. R. Sabin, N. N. Gerasimchuk, V. N. Nemykin, *J. Porphyrins Phthalocyanines* **2011**, *15*, 612; c) E. R. Baral, D. Kim, S. Lee, M. H. Park, J. G. Kim, *CSD Communication*, *CCDC 1964150*, **2019**; d) S. Prasad, M. Bhadbhade, P. Thordarson, *CSD Communication*, *CCDC 759436*, **2012**; e) J. Jiang, X. Jin, C. Li, Z. Gu, *J. Coord.* **1995**, *35*, 313; f) E. Giannoudis, E. Benazzi, J. Karlsson, G. Copley, S. Panagiotakis, G. Landrou, P. Angaridis, V. Nikolaou, C. Matthaiaki, G. Charalambidis, *CSD Communication*, *CCDC 1935835*, **2020**.
[21] S. Lipstman, I. Goldberg, *CSD Communication*, *CCDC 795766*, **2011**.

[22] S. L. Tong, J. Zhang, Y. Yan, S. Hu, J. Yu, L. Yu, *Solid State Sci.* **2011**, *13*, 1320.
[23] R. Soman, D. Raghav, S. Sujatha, K. Rathinasamy, C. Arunkumar, *RSC Adv.* **2015**, *5*, 61103.
[24] D. M. Collins, W. R. Scheidt, J. L. Hoard, *J. Am. Chem. Soc.* **1972**, *94*, 6689.
[25] J. S. Lindsey, *Catalysis by Metal Complexes, Vol. 17*, Springer Netherlands, Dordrecht, s.l., **1994**, pp. 49–86.
[26] J. S. Lindsey, R. W. Wagner, *J. Org. Chem.* **1989**, *54*, 828.
[27] S. Stadlbauer, *PhD Thesis*, TU Graz, **2019**.
[28] M. O. Senge, I. Bischoff, N. Y. Nelson, K. M. Smith, *J. Porphyrins Phthalocyanines* **1999**, *03*, 99.
[29] a) W. M. Campbell, K. W. Jolley, P. Wagner, K. Wagner, P. J. Walsh, K. C. Gordon, L. Schmidt-Mende, M. K. Nazeeruddin, Q. Wang, M. Grätzel, *J. Phys. Chem. C* **2007**, *111*, 11760; b) G. R. Geier, J. S. Lindsey, *Tetrahedron* **2004**, *60*, 11435.
[30] M. El Abbassi, P. Zwick, A. Rates, D. Stefani, A. Prescimone, M. Mayor, H. S. J. van der Zant, D. Dulić, *Chem. Sci.* **2019**, *10*, 8299.
[31] a) J. F. F. Jose-Larong, Y. Takahashi, T. Inabe, *Struct. Chem.* **2013**, *24*, 113; b) P. W. Codding, A. Tulinsky, *J. Am. Chem. Soc.* **1972**, *94*(12), 4151; c) N. Grover, P. Rathi, M. Sankar, *J. Porphyrins Phthalocyanines* **2015**, *19*, 997; d) M. S. Somma, C. J. Medforth, N. Y. Nelson, M. M. Olmstead, R. G. Khoury, K. M. Smith, *Chem. Commun.* **1999**, *13*, 1221; e) M. O. Senge, S. Runge, *Acta Crystallogr. Sect. C* **1998**, *54*, 1917; f) R. Plamont, Y. Kikkawa, M. Takahashi, M. Kanesato, M. Giorgi, A. Chan Kam Shun, C. Roussel, T. S. Balaban, *Chem.* **2013**, *19*, 11293; g) G. Donnay, C. B. Storm, *Mol. Cryst.* **1967**, *2*, 287; h) K. Kano, K. Fukuda, H. Wakami, R. Nishiyabu, R. F. Pasternack, *J. Am. Chem. Soc.* **2000**, *122*, 7494; i) M. J. Hamor, T. A. Hamor, J. L. Hoard, *J. Am. Chem. Soc.* **1964**, *86*(10) 1938; j) C. Brückner, J. Ogikubo, J. R. McCarthy, J. Akhigbe, M. A. Hyland, P. Daddario, J. L. Worlinsky, M. Zeller, J. T. Engle, C. J. Ziegler, *J. Org. Chem.* **2012**, *77*, 6480; k) Z. Li, Y. Hu, T. Li, *Mol. Cryst.* **2014**, *605*, 135; l) M. P. Byrn, C. J. Curtis, I. Goldberg, Y. Hsiou, S. I. Khan, P. A. Sawin, S. K. Tendick, C. E. Strouse, *J. Am. Chem. Soc.* **1991**, *113*, 6549; m) M. P. Byrn, C. J. Curtis, S. I. Khan, P. A. Sawin, R. Tsurumi, C. E. Strouse, *J. Am. Chem. Soc.* **1990**, *112*, 1865; n) G. L. Perlovich, W. Zielenkiewicz, Z. Kaszkur, J. Słowikowska, *J. Mol. Liq.* **2002**, *95*, 243; o) P. D. W. Boyd, M. C. Hodgson, C. E. F. Rickard, A. G. Oliver, L. Chaker, P. J. Brothers, R. D. Bolskar, F. S. Tham, C. A. Reed, *J. Am. Chem. Soc.* **1999**, *121*, 10487; p) J. Blömker, W. Frey, *Z. Kristallogr. N. Cryst.* **2000**, *215*, 267; q) R. J. Butcher, G. B. Jameson, C. B. Storm, *J. Am. Chem. Soc.* **1985**, *107*, 2978; r) R. Soman, S. Sujatha, C. Arunkumar, *J. Porphyrins Phthalocyanines* **2016**, *20*, 833; s) G. Lu, X. Zhang, X. Cai, Y. Fang, M. Zhu, W. Zhu, Z. Ou, K. M. Kadish, *J. Porphyrins Phthalocyanines* **2013**, *17*, 941; t) P. Ochsenbein, K. Ayougou, D. Mandon, J. Fischer, R. Weiss, R. N. Austin, K. Jayaraj, A. Gold, J. Terner, J. Fajer, *Angew. Chem. Int. Ed.* **1994**, *33*, 348; u) N. Sheng, S. Zong, W. Cao, J. Jiang, Z. Wang, Y. Cui, *ACS Appl. Mater. Interfaces* **2015**, *7*, 19718.
[32] S. K. Nayak, R. Sathishkumar, T. N. G. Row, *CrystEngComm* **2010**, *12*, 3112.
[33] E. A. Meyer, R. K. Castellano, F. Diederich, *Angew. Chem. Int. Ed.* **2003**, *42*, 1210.
[34] a) C. Janiak, *J. Chem. Soc. Dalton Trans.* **2000**, *21*, 3885; b) C. A. Hunter, J. K. M. Sanders, *J. Am. Chem. Soc.* **1990**, *112*, 5525.
[35] a) V. Balamurugan, W. Jacob, J. Mukherjee, R. Mukherjee, *CrystEngComm* **2004**, *6*, 396; b) V. Balamurugan, M. S. Hundal, R. Mukherjee, *Chem.* **2004**, *10*, 1683; c) A. Nangia, *CrystEngComm* **2002**, *4*, 93; d) C. B. Aakeröy, T. A. Evans, K. R. Seddon, I. Pálinkó, *New J. Chem.* **1999**, *23*, 145.
[36] R. D. Willett, B. Twamley, W. Montfrooij, G. E. Granroth, S. E. Nagler, D. W. Hall, J.-H. Park, B. C. Watson, M. W. Meisel, D. R. Talham, *Inorg. Chem.* **2006**, *45*, 7689.
[37] Y. V. Nelyubina, M. Y. Antipin, K. A. Lyssenko, *J. Phys. Chem.* **2007**, *111*, 1091.
[38] S. Alvarez, *Dalton Trans.* **2013**, *42*, 8617.
[39] S. Lipstman, I. Goldberg, *Cryst. Growth Des.* **2010**, *10*, 4596.
[40] W. Sinha, M. Kumar, A. Garai, C. S. Purohit, T. Som, S. Kar, *Dalton Trans.* **2014**, *43*, 12564.
[41] Bruker APEX2 and SAINT, Bruker AXS Inc.: Madison, Wisconsin, USA, **2012**.
[42] G. M. Sheldrick, "Cell_Now. Program to isolate multiple orientations for crystals suffering from non-merohedral twinning." **2008**.
[43] a) R. H. Blessing, *Acta Crystallogr. Sect. A* **1995**, *51(Pt1)*, 33; b) G. M. Sheldrick, SADABS, Version 2.10, Siemens Area Detector Correction, Universität Göttingen, Germany, **2003**.
[44] G. M. Sheldrick, *Acta Crystallogr. Sect. A* **2015**, *71*(1), 3–8.
[45] a) G. M. Sheldrick, *Acta Crystallogr. Sect. A* **1990**, *46(6)*, 467-473; b) G. M. Sheldrick, *Acta Crystallogr. Sect. A* **2008**, *64*(1), 112-122; c) G. M. Sheldrick, *Acta Crystallogr. Sect. C* **2015**, *71*(1), 3-8; d) Sheldrick, G. M. SHELXS97, Univ. Göttingen, Germany, **1997**.
[46] C. B. Huebschle, G. M. Sheldrick, B. Dittrich *J. Appl. Crystallogr.* **2011**, *44*, 1281.
[47] a) A. L. Spek, *J. Appl. Crystallogr.* **2003**, *36*, 7; b) A. L. Spek, *Acta Crystallogr. Sect. D* **2009**, *65*, 148.
[48] A. L. Spek, *Acta Crystallogr. Sect. C* **2015**, *71*(1), 9–18.
[49] P. Müller, R. Herbst-Irmer, A. L. Spek, T. R. Schneider, M. R. Sawaya, *Crystal Structure Refinement*: A Crystallographer's Guide to SHELXL Oxford University Press: **2006**, p 232.
[50] P. van der Sluis, A. L. Spek, *Acta Crystallogr. Sect. A* **1990**, *46*, 194.
[51] H. Putz, Brandenburg, K. Diamond - Crystal and Molecular Structure Visualization, 4.6.5, G. Crystal Impact: Bonn.
[52] F. H. Allen, O. Johnson, G. P. Shields, B. R. Smith, M. Towler, *J. Appl. Crystallogr.* **2004**, *37*, 335.
[53] S. P. Westrip, *J. Appl. Crystallogr.* **2010**, *43*, 920.
[54] O. V. Dolomanov, L. J. Bourhis, R. J. Gildea, J. A. K. Howard, H. Puschmann, *J. Appl. Crystallogr.* **2009**, *42*, 339.
[55] a) C. Janiak, *Dalton Trans.* **2000**, *21*, 3885–3896; b) C. A. Hunter, J. K. M. Sanders, *J. Am. Chem. Soc.* **1990**, *112*(14) 5525-5534.
[56] C. F. Macrae, I. J. Bruno, J. A. Chisholm, P. R. Edgington, P. McCabe, E. Pidcock, L. Rodriguez-Monge, R. Taylor, J. van de Streek, P. A. Wood, *J. Appl. Crystallogr.* **2008**, *41*, 466.

Manuscript received: May 15, 2023
Revised manuscript received: July 27, 2023
Accepted manuscript online: July 28, 2023
Version of record online: August 14, 2023